Received: 29 February 2024 | Revised: 29 May 2024 | Accepted: 5 June 2024

DOI: 10.1111/cas.16254

ORIGINAL ARTICLE

Cancer Science WILEY

Methyltransferase like-14 suppresses growth and metastasis of non-small-cell lung cancer by decreasing LINC02747

Jiemin Wang | Shu Wang | Haopeng Yang | Ruixuan Wang | Kesong Shi | Yueshi Liu | Le Dou | Haiquan Yu

State Key Laboratory of Reproductive Regulation and Breeding of Grassland Livestock, School of Life Sciences, Inner Mongolia University, Hohhot, Inner Mongolia, China

Correspondence
Haiquan Yu, State Key Laboratory of Reproductive Regulation and Breeding of Grassland Livestock, School of Life Sciences, Inner Mongolia University, Hohhot 010020, Inner Mongolia, China.
Email: hyu@imu.edu.cn

Funding information
Science and Technology Program of the Joint Fund of Scientific Research for the Public Hospitals of Inner Mongolia Academy of Medical Sciences, Grant/Award Number: 2023GLLH0037; Key Technology Research Plan Project of Inner Mongolia Autonomous Region, Grant/Award Number: 2021GG0153

Abstract

Multiple epigenetic regulatory mechanisms exert critical roles in tumor development, and understanding the interactions and impact of diverse epigenetic modifications on gene expression in cancer is crucial for the development of precision medicine. We found that methyltransferase-like 14 (METTL14) was significantly downregulated in non-small-cell lung cancer (NSCLC) tissues. Functional experiments demonstrated that overexpression of METTL14 inhibited the proliferation and migration of NSCLC cells both in vivo and in vitro, and the colorimetric m^6A quantification assay also showed that knockdown of METTL14 notably reduced global m^6A modification levels in NSCLC cells. By using the methylated-RNA immunoprecipitation-qPCR and dual-luciferase reporter assays, we verified that long noncoding RNA LINC02747 was a target of METTL14 and was regulated by METTL14-mediated m^6A modification, and silencing LINC02747 inhibited the malignant progression of NSCLC by modulating the PI3K/Akt and CDK4/Cyclin D1 signaling pathway. Further studies revealed that overexpression of METTL14 promoted m^6A methylation and accelerated the decay of LINC02747 mRNA via increased recognition of the "GAACU" binding site by YTHDC2. Additionally, histone demethylase lysine-specific histone demethylase 5B (KDM5B) mediated the demethylation of histone H3 lysine 4 tri-methylation (H3K4me3) in the METTL14 promoter region and repressed its transcription. In summary, KDM5B downregulated METTL14 expression at the transcriptional level in a H3K4me3-dependent manner, while METTL14 modulated LINC02747 expression via m^6A modification. Our results demonstrate a synergy of multiple mechanisms in regulating the malignant phenotype of NSCLC, revealing the complex regulation involved in the occurrence and development of cancer.

KEYWORDS
histone modification, LINC02747, m^6A modification, METTL14, non-small-cell lung cancer

Jiemin Wang and Shu Wang contributed equally to this work.

1 | INTRODUCTION

Non-small-cell lung cancer (NSCLC) accounts for about 85% of all lung cancers and can be further categorized into adenocarcinoma (LUAD), squamous cell carcinoma (LUSC), and large-cell lung cancer.[1] Despite considerable progress in the identification and treatment of NSCLC in recent years, the rates of early detection, overall recovery, and survival remain less than satisfactory, particularly in cases of metastatic NSCLC.[2]

Epigenetics is a multifaceted field that involves the investigation of reversible and heritable molecular alterations that influence gene transcription and phenotype. At the forefront of this discipline are processes such as DNA and RNA methylation, histone modifications, noncoding RNA-associated alterations, and chromatin structural dynamics. Among these epigenetic modifications, N^6-methyladenosine (m^6A) RNA modifications act as a regulatory nexus that modulates gene expression critical to cancer pathogenesis and progression.[3,4] m^6A modifications are catalyzed by methyltransferases, called "writers", and the dynamic and reversible nature of m^6A modifications is attributed to "eraser" demethylases that can remove m^6A marks. Moreover, specific "reader" proteins recognize m^6A modifications and mediate their effects.[5–8]

m^6A methyltransferase methyltransferase-like 14 (METTL14) is the core of the m^6A methyltransferase complex and participates in the regulation of tumor proliferation, metastasis, and self-renewal, affecting tumorigenesis and tumor progression. It has been reported that METTL14 promotes hepatocellular carcinoma metastasis by regulating DGCR8 in the nucleus and thereby decreasing miR-126 expression.[9] Recent research highlights the synergistic interactions among different epigenetic processes during cancer progression. For example, in our prior research on lung adenocarcinoma cells, it was shown that reducing METTL3 levels led to an increase in the expression of the histone methylase SET-domain-containing 2 and a higher count of histone H3 lysine 36 trimethylation (H3K36me3) marks in the transcript's promoter region.[3] The interplay between these epigenetic mechanisms adds complexity to cancer diagnosis and treatment, and elucidating these mechanisms can aid the development of novel therapeutic strategies.

This study focused on exploring the function of METTL14 in NSCLC and its effect on regulating target molecules. By analyzing its downstream target genes and upstream regulatory molecules, we discovered that histone demethylase lysine-specific histone demethylase 5B (KDM5B) downregulated METTL14 expression in a histone H3 lysine 4 tri-methylation (H3K4me3)-dependent manner, while METTL14 regulated LINC02747 expression via m^6A modification. This correlation between METTL14-mediated m^6A alterations and histone modifications in NSCLC provides new insights for cancer therapy.

2 | MATERIALS AND METHODS

Detailed materials and methods including tissue samples and patients, data sources and bioinformatics analysis, cell lines and cell culture, qRT–PCR, transient transfection and lentiviral infection, immunohistochemistry, Western blot analysis, cell proliferation and migration assay, flow cytometry assay, animal experiments, N^6-methyladenosine quantification assay, RNA immunoprecipitation (RIP) and methylated-RNA immunoprecipitation assays, luciferase reporter assay, RNA stability assay, chromatin immunoprecipitation (ChIP) assay, Northern blot analysis, and statistical analysis are provided in Appendix S1.

3 | RESULTS

3.1 | METTL14 is downregulated in NSCLC and associated with a poorer prognosis

To ascertain the role of METTL14 in NSCLC, we initially assessed METTL14 expression levels in NSCLC. We found that METTL14 expression was significantly downregulated in NSCLC tissues, as observed in both the cancer genome atlas (TCGA) (LUAD and LUSC) and gene expression omnibus (GEO) (GSE40791 and GSE81889) datasets (Figure 1A,B). Then, the expression of METTL14 was confirmed in NSCLC tissues by qRT–PCR (Figure 1C). The primer sequences are shown in Table S1. Accordingly, immunohistochemistry was performed to determine METTL14 expression at the protein level, and the results showed that METTL14 expression was significantly lower in NSCLC tissue samples ($n=95$) than in paired normal tissue samples ($n=81$) (Figure 1D). In addition, downregulated METTL14 expression was associated with tumor size, TNM stage and EGFR expression in patients with NSCLC (Table 1). K–M analysis of our cohort demonstrated that low METTL14 expression was correlated with poor patient survival (Figure 1E). The results from another independent TCGA cohort were consistent, confirming poor progression-free survival (PFS) and overall survival (OS) in NSCLC patients with low METTL14 expression (Figure 1F,G). Furthermore, multivariate and receiver operating characteristic (ROC) analyses revealed that METTL14 expression was an independent prognostic factor in NSCLC patients (Figure 1H,I). Moreover, we analyzed the RNA-seq data of NSCLC cells (A549, H1299, H1975, and H460) and control cells (BEAS-2B). The findings indicated that METTL14 was significantly downregulated in these NSCLC cell types compared to BEAS-2B cells (Figure 1J). Consistent with the GEO database, qRT–PCR and Western blot analysis further confirmed that METTL14 was decreased in A549, H1299, H1975 and H460 cells compared to BEAS-2B cells (Figure 1K,L). Collectively, these results indicated that METTL14 was significantly downregulated in NSCLC and might be associated with NSCLC progression.

3.2 | METTL14 inhibits the proliferation, cell cycle progression, and migration of NSCLC cells in vitro

To investigate the role of METTL14 in NSCLC, we transfected A549 and H460 cells with two siRNAs targeting METTL14 (siRNA sequences are shown in Table S2), and the efficacy of the knockdown

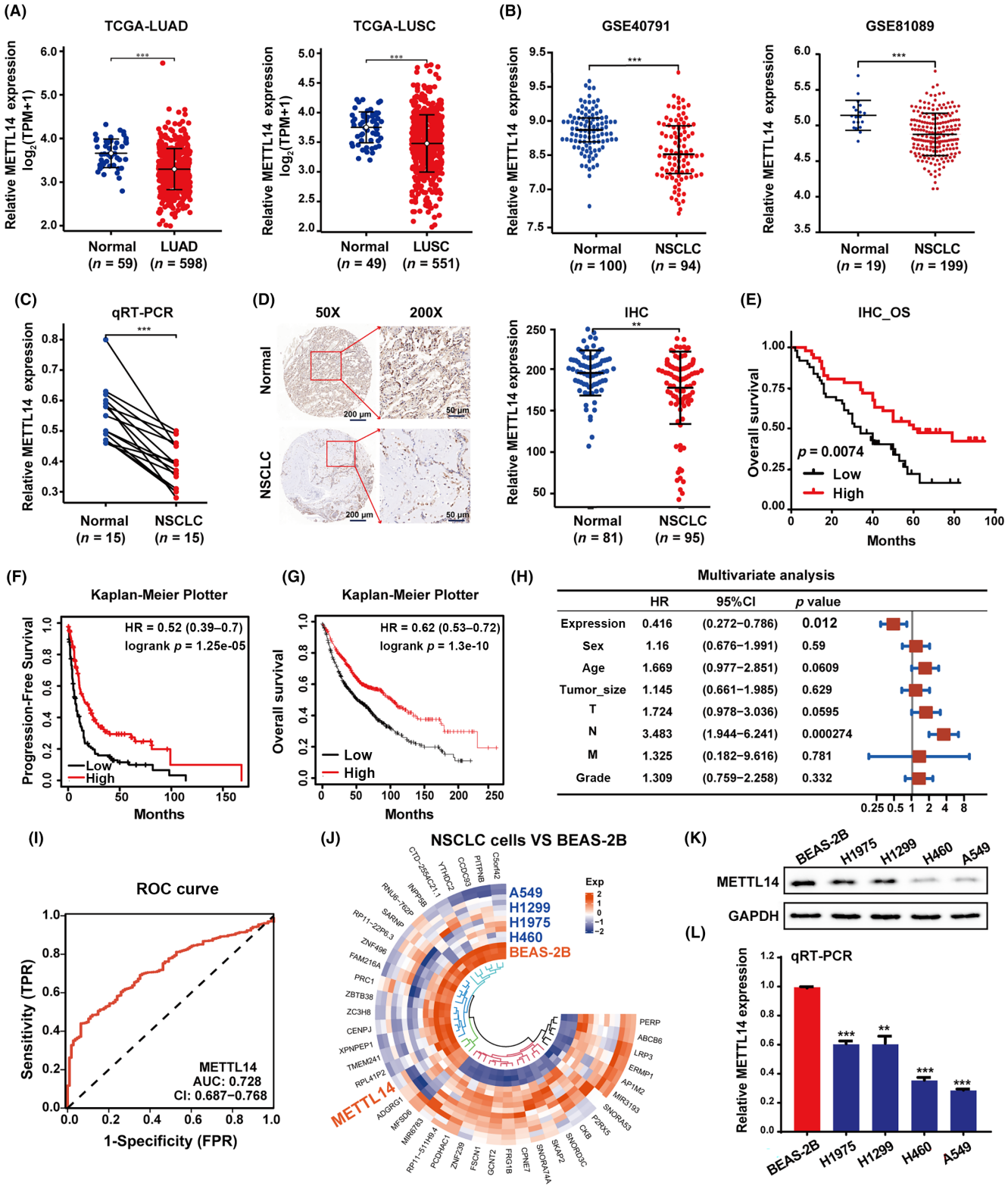

FIGURE 1 METTL14 expression is downregulated in NSCLC and is associated with patient prognosis. (A) METTL14 mRNA expression levels were analyzed using RNA-seq data from the TCGA-LUAD and TCGA-LUSC cohorts. (B) METTL14 expression levels in the NSCLC cohorts from GSE40791 and GSE81089. (C) The expression of METTL14 in 15 NSCLC tissues and paracancerous tissues was detected by qRT–PCR. (D) IHC analysis of METTL14 protein expression in 95 NSCLC tissues and 81 paracancerous tissues. (E) Analysis of the relationship between METTL14 expression and overall survival (OS) in NSCLC patients based on IHC results ($P < 0.01$, log-rank test). (F, G) Progression-free survival (F) and overall survival (G) based on METTL14 expression levels in NSCLC patients analyzed using the Kaplan–Meier plotter. (H) Multivariate analysis of factors associated with OS in 95 NSCLC patients. All bars correspond to the 95% CI. (I) TCGA database analysis of ROC curves of METTL14. (J) Differentially expressed genes in NACLC and BEAS-2B cells. (K, L) The expression of METTL14 in NSCLC cells and BEAS-2B cells was detected using Western blot (K) and qRT–PCR (L). Error bars = mean ± SD. $^{**}P < 0.01$, $^{***}P < 0.001$.

TABLE 1 Clinical characteristics of 95 NSCLC patients according to METTL14 protein levels.

Variables	METTL14 expression		Total	*P* value	X^2
	Low ($n=49$)	High ($n=46$)			
Sex				0.8015	0.0632
Male	30	27	57		
Female	19	19	38		
Age (years)				0.6921	0.1269
≤60	20	23	43		
>60	25	27	52		
Grade				0.3145	1.0115
I/II	27	30	57		
III	22	16	38		
Tumor size				0*	16.678
≤4 cm	18	36	54		
>4 cm	31	10	41		
T stage				0.0017*	9.8809
T1/T2	30	37	72		
T3/T4	19	4	23		
N stage				0.2627	1.2543
N0	21	25	46		
N1–N3	28	21	49		
TNM stage				0.0456*	3.9964
I/II	29	36	65		
III/IV	20	10	30		
EGFR				0.0198*	5.4258
Negative	29	30	59		
Positive	11	2	13		
PDL1				0.7672	0.0877
≤2.5	32	11	43		
>2.5	25	10	35		

*Statistically significant values.

was confirmed by Western blotting and qRT–PCR (Figure 2A,B). The proliferation of NSCLC cells was markedly increased following the knockdown of METTL14 expression (Figure 2C). Subsequent flow cytometry analysis revealed that METTL14 knockdown resulted in a lower percentage of NSCLC cells in the G0/G1 phase and a higher percentage in the S phase (Figure 2D). Cyclin D1 binds to CDK4 to form a heterodimeric complex that controls the transition from the G1 phase to the S phase, which initiates DNA replication.[10,11] Mechanistically, we found that the knockdown of METTL14 led to an upregulation in the expression levels of both CDK4 and Cyclin D1 (Figure 2E). Additionally, transwell assay results indicated a substantial increase in the migration of NSCLC cells following METTL14 knockdown (Figure 2F). Furthermore, METTL14 overexpression (OE-METTL14) and a control lentivirus (OE-NC) were engineered and transfected into NSCLC cells (Figure 2G,H). As expected, upregulating METTL14 expression led to a decrease in cell proliferation (Figure 2I), cell cycle progression (Figure 2J), and cell migration (Figure 2L) in A549 and H460 cells. In addition, there was a reduction in the protein levels of Cyclin D1 and CDK4 subsequent to the overexpression of METTL14 (Figure 2K).

3.3 | METTL14 suppresses tumor growth and metastasis in vivo

To further investigate the effects of METTL14 expression in vivo, we constructed H460 cells stably overexpressing METTL14 and subcutaneously injected them into the armpits of mice (Figure 3A). The resulting tumors exhibited smaller volumes (Figure 3B) and lower weights (Figure 3C) than those in the control group, as observed 21 days post injection. Additionally, the expression of Ki67 was downregulated in the smaller xenografts (Figure 3D). Furthermore, the impact of METTL14 on NSCLC metastasis was evaluated by conducting tail vein injections in BALB/c nude mice (Figure 3E). The outcomes showed that overexpressing METTL14 markedly reduced NSCLC cell metastasis within a period of 6 weeks, which was confirmed by fewer lung metastatic nodules being observed (Figure 3F). Summarily, these results suggest that increasing METTL14 levels suppresses both tumor growth and metastasis of NSCLC cells in a living organism.

3.4 | METTL14 inhibits NSCLC malignancy through the LINC02747-mediated PI3K/Akt signaling pathway

We then explored how METTL14 reduces the malignancy of NSCLC cells. As a crucial m^6A methyltransferase, METTL14 is capable of attaching methyl groups to m^6A sites on specific RNAs, which in turn triggers downstream signaling pathways. To identify potential RNAs interacting with METTL14 possibly through m^6A modification, we downloaded the gene set GSE54365 from the RM2Target database, which includes Me-RIP-seq data from A549 cells with METTL14 knockout. The screening criteria were $\log_2$-fold change $>|2|$ and P value <0.01. We identified 12 potential target RNAs (Table S3). Subsequently, the correlation between these potential target RNAs and the expression of METTL14 in NSCLC tissues was analyzed using data from the TCGA database (Figure 4A). The qRT–PCR results showed an increase in LINC02747 expression in NSCLC cells with METTL14 knockdown and a decrease in cells with METTL14 overexpression (Figures 4B and S1A,B). RIP–qPCR analysis confirmed the strong binding of METTL14 to LINC02747 (Figure 4C). We conducted an analysis of LINC02747 expression in NSCLC tissues using the TCGA database and revealed a notable upregulation in its expression (Figure S2A,B). Gene Set Enrichment Analysis (GSEA) of the TCGA-LUAD and TCGA-LUSC datasets showed that LINC02747 was positively associated with the cell cycle and PI3K/

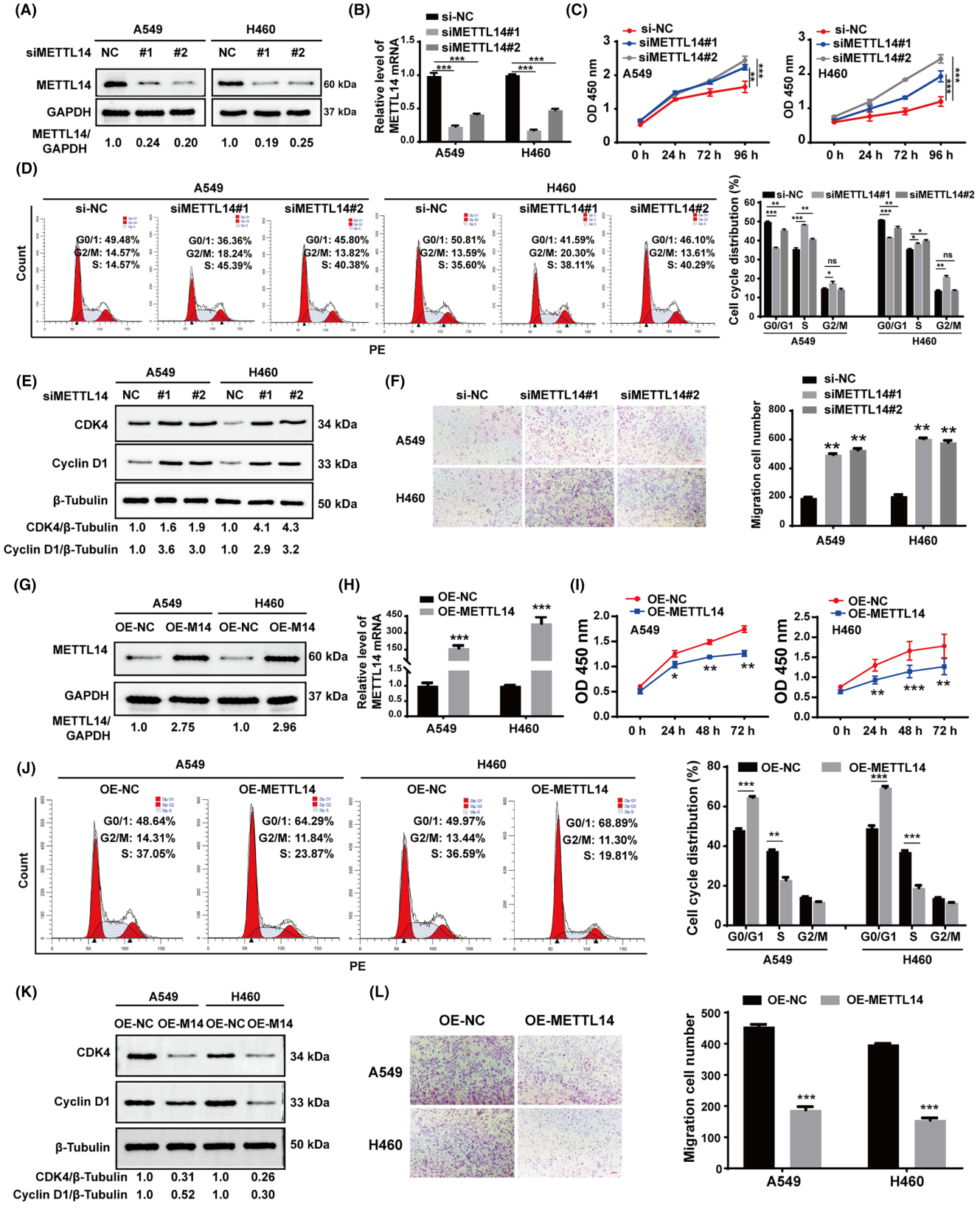

FIGURE 2 METTL14 inhibits NSCLC cell proliferation, cell cycle progression and migration in vitro. (A, B) The knockdown efficiency of METTL14 at the protein (A) and mRNA levels (B) after transfection of METTL14 siRNA in NSCLC cells. (C, D, F) CCK-8 assay (C), flow cytometry assay (D), and transwell assay (F) of NSCLC cells transfected with METTL14 siRNAs or si-NC. (E) The protein levels of CDK4 and Cyclin D1 in NSCLC cells transfected with METTL14 siRNAs. (G, H) The overexpression efficiency of METTL14 at the protein (G) and mRNA (H) levels after transfection of METTL14 pcDNA3.1 (OE-METTL14) or pcDNA3.1 (OE-NC). (I, J, L) CCK-8 assay (I), flow cytometry assay (J), and transwell assay (L) of METTL14-overexpressing and control NSCLC cells. (K) The protein levels of CDK4 and Cyclin D1. Error bars = mean ± SD. $^{*}P < 0.05$, $^{**}P < 0.01$, $^{***}P < 0.001$.

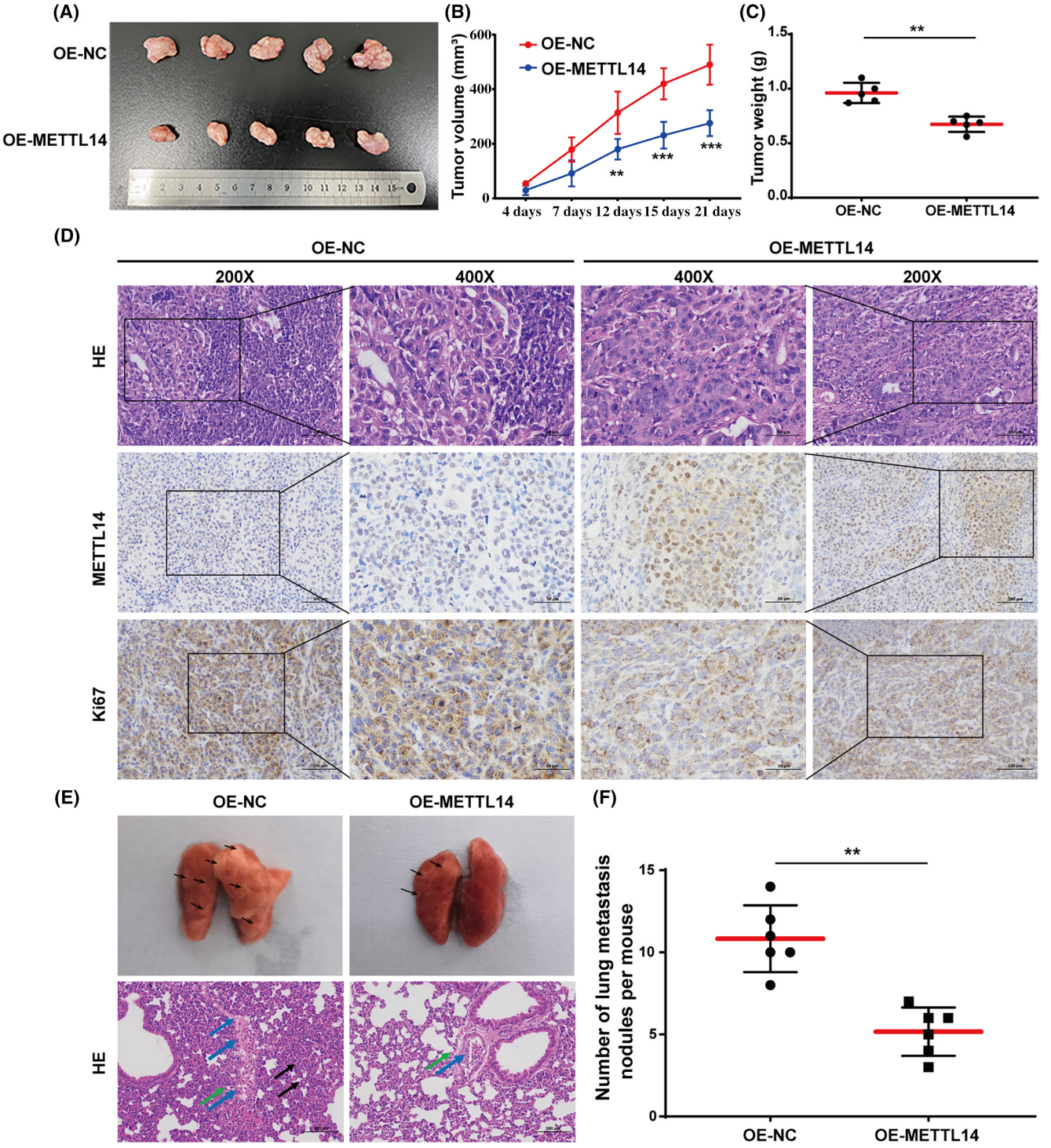

FIGURE 3 METTL14 suppresses tumor growth and metastasis in vivo. (A) Subcutaneous xenograft tumor model in mice overexpressing METTL14. (B, C) Tumor growth curves (B) and tumor weights in the METTL14-overexpressing and control groups. (D) METTL14 and KI67 expression was determined via IHC. Scale bar, 200×, 100 μm; 400×, 50 μm. (E, F) Representative images of a nude mouse lung metastasis model overexpressing METTL14. H&E staining (E) and the number of lung metastatic nodules was determined (F). Scale bar, 100 μm. Error bars = mean ± SD. $^{**}P < 0.01$, $^{***}P < 0.001$.

Akt pathway in LUAD and LUSC (Figure 4D). Additionally, qRT–PCR analysis demonstrated a significant increase in LINC02747 expression in NSCLC tissues compared to paracancerous tissues (Figure 4E). Moreover, there was a negative correlation between the expression levels of LINC02747 and METTL14 (Figure 4F).

Previous reports have indicated that LINC02747 enhances the development of clear cell renal cell carcinoma.[12] In our study, we observed an increase in LINC02747 expression in NSCLC cells (Figure S2C). Disruption of LINC02747 expression led to reduced proliferation, cell cycle progression, and migration in NSCLC cells

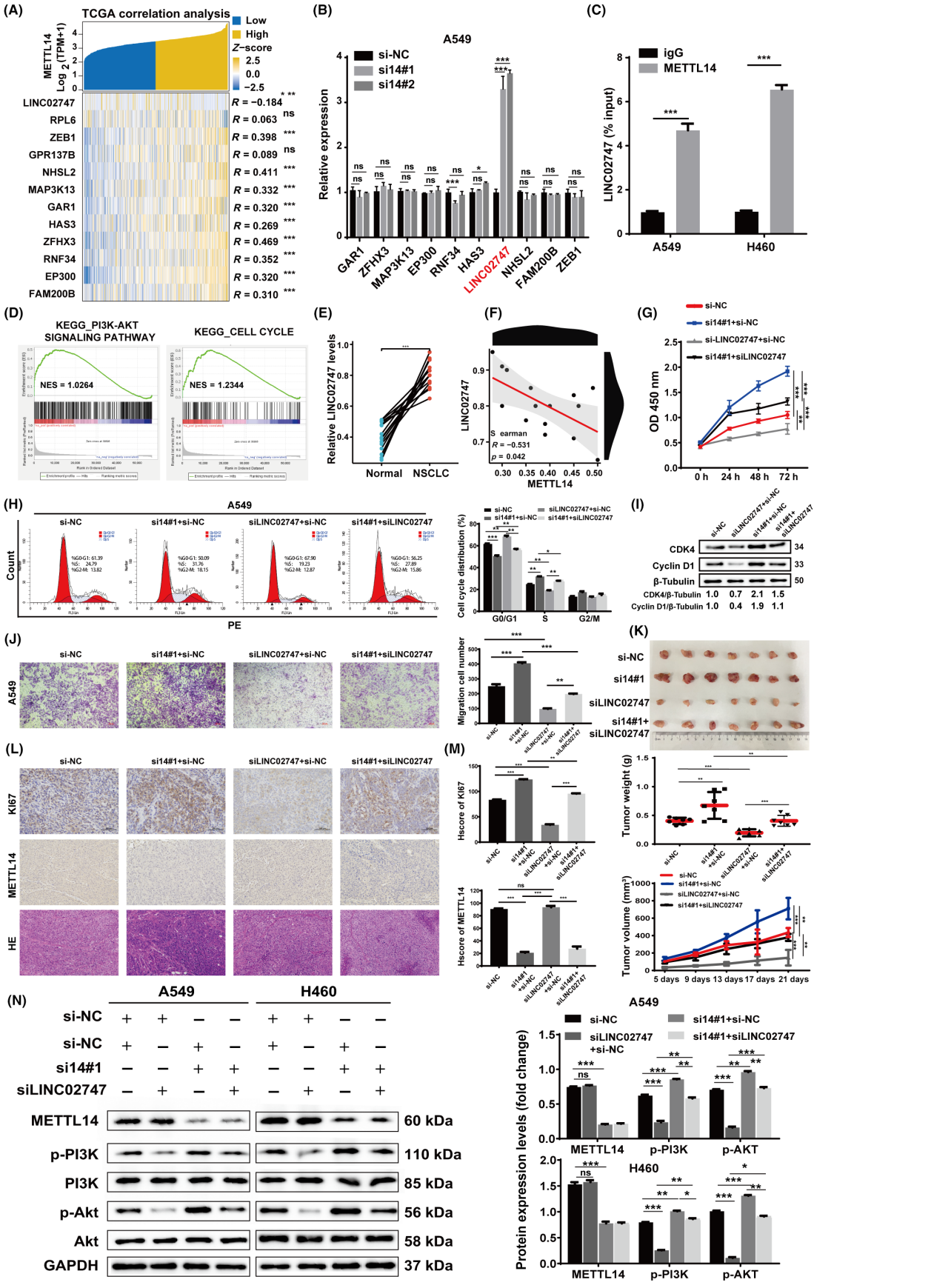

FIGURE 4 Legend on next page

FIGURE 4 METTL14 inhibits NSCLC malignancy through the LINC02747-mediated PI3K/Akt signaling pathway. (A) METTL14 correlations with candidate target genes were analyzed in the TCGA database. (B) The mRNA levels of target genes after METTL14 knockdown in A549 cells were analyzed via qRT–PCR. (C) RIP–qPCR results showing that METTL14 binds to LINC02747. (D) GSEA enrichment analysis of LINC02747 in the TCGA database. (E) The expression of LINC02747 in 15 NSCLC tissues and paracancerous tissues was detected by qRT–PCR. (F) Correlation analysis of METTL14 and LINC02747 in 15 NSCLC tissues. (G, H, J) CCK-8 (G), flow cytometry (H) and transwell assays (J) for METTL14 and LINC02747 rescue analysis. (I) Detection of protein levels of CDK4 and Cyclin D1. (K) In vivo appearance of tumor formation in nude mice (top right), growth curves of tumors (bottom left) and weight (bottom right). (L) IHC was performed to detect the expression of KI67. Scale bar, 100 μm. (M) H-score of KI67. (N) Western blot detection of the PI3K/Akt pathway. Error bars = mean ± SD. $^{*}P < 0.05$, $^{**}P < 0.01$, $^{***}P < 0.001$.

(Figure S2D–H). Furthermore, Western blot results revealed that the reduction of LINC02747 lowered the phosphorylation levels of PI3K and Akt proteins (Figure S2I), indicating that LINC02747 may activate the PI3K/Akt signaling pathway.

To elucidate the involvement of LINC02747 in the METTL14-mediated suppression of the malignant phenotype in NSCLC, we employed siRNA targeting LINC02747 to silence its expression in METTL14-knockdown NSCLC cells. The findings indicated that silencing LINC02747 considerably reduced the increase in NSCLC cell proliferation, cell cycle advancement, and migration that was initially stimulated by the knockdown of METTL14 (Figures 4G,H,J and S3A,B,D). Mechanistically, silencing LINC02747 abrogated the upregulation of CDK4 and Cyclin D1 proteins induced by METTL14 knockdown (Figures 4I and S3C). Experimental results from in vivo studies showed that mice with knocked down METTL14 had significantly larger and heavier tumors compared to those in the control group. However, downregulating LINC02747 inhibited the tumor progression induced by METTL14 knockdown (Figure 4K). Immunohistochemical analysis further indicated that the knockdown of METTL14 led to an increased expression of Ki67, which was reversed on the reduction of LINC02747 levels (Figure 4L,M). Additionally, Western blot analysis showed that the knockdown of METTL14 promoted the phosphorylation of PI3K and Akt proteins, indicating the activation of the PI3K/Akt signaling pathway. Inhibiting the expression of LINC02747 reversed this activation (Figure 4N). Taken together, our findings revealed that METTL14 exerts its biological function by regulating the LINC02747-mediated PI3K/Akt pathway.

3.5 | METTL14 regulates LINC02747 expression through m^{6}A modification

We then verified if METTL14 directly influences the reduction of LINC02747 expression in an m^{6}A-dependent manner. By conducting a colorimetric m^{6}A quantification assay on NSCLC cells, it was observed that METTL14 knockdown lowered m^{6}A levels in these cells (Figure 5A), whereas its overexpression increased m^{6}A levels (Figure 5B). Additionally, according to MeRIP-seq data (GSE55572), the abundance of m^{6}A in LINC02747 was reduced in A549 cells with METTL14 knocked out compared to control cells (Figure 5C), and we also observed a general decrease in the m^{6}A abundance across all genes (Figure 5D). Using the SRAMP online site, we predicted a high-scoring m^{6}A modification site in the LINC02747 sequence (Figure 5E). Subsequently, MeRIP–qPCR validated a significant decrease in m^{6}A abundance at this site with METTL14 knockdown, while its overexpression markedly increased m^{6}A abundance (Figure 5F). Furthermore, luciferase reporter vectors for wild-type or mutant LINC02747 were constructed to assess the effect of m^{6}A modification on LINC02747 expression (Figure 5G). Dual luciferase assays showed that overexpression of METTL14 decreased the luciferase activity of wild-type LINC02747, but its mutant showed no significant change in luciferase activity (Figure 5H). These findings indicate that METTL14 methylates the m^{6}A site of LINC02747 to regulate its expression in NSCLC cells.

3.6 | Overexpression of METTL14 accelerates the degradation of LINC02747 mRNA via an m^{6}A-YTHDC2-dependent pathway

Methylation of m^{6}A is a marking process that necessitates identification by m^{6}A "readers" to exert its effects on the target RNAs.[13] Our analysis of the TCGA database revealed a significant association between LINC02747 and m^{6}A readers YTHDC2, IGF2BP2, and IGF2BP3 (Figure 6A). In both A549 and H460 cell lines, we observed a suppression of these three m^{6}A readers (Figure S4A). Notably, only the suppression of YTHDC2 led to an increase in LINC02747 levels (Figure 6B). YTHDC2 expression was downregulated in NSCLC tissues in the TCGA dataset results, which was consistent with our experiments (Figure S4B–D). Furthermore, qRT–PCR analysis

FIGURE 5 METTL14 negatively regulates LINC02747 in a m^{6}A-dependent manner. (A, B) The m^{6}A levels in total RNA from NSCLC cells after overexpression of METTL14 or knockdown of METTL14 were determined using a colorimetric assay. (C) Enrichment of LINC02747 in A549 knockdown MeRIP-seq data of METTL14. (D) Signal distribution of m^{6}A in transcripts. (E) The SRAMP website was used to predict the m^{6}A modification site on LINC02747. (F) Determination of LINC02747 m^{6}A modification levels after knockdown (left) or overexpression (right) of METTL14 in NSCLC cells using MeRIP–qPCR. (G) The schematic shows the m^{6}A methylation site at 2175 bp on LINC02747, which was mutated. (H) Dual luciferase reporter assay for LINC02747 and METTL14. Error bars = mean ± SD. $^{*}P < 0.05$, $^{**}P < 0.01$, $^{***}P < 0.001$.

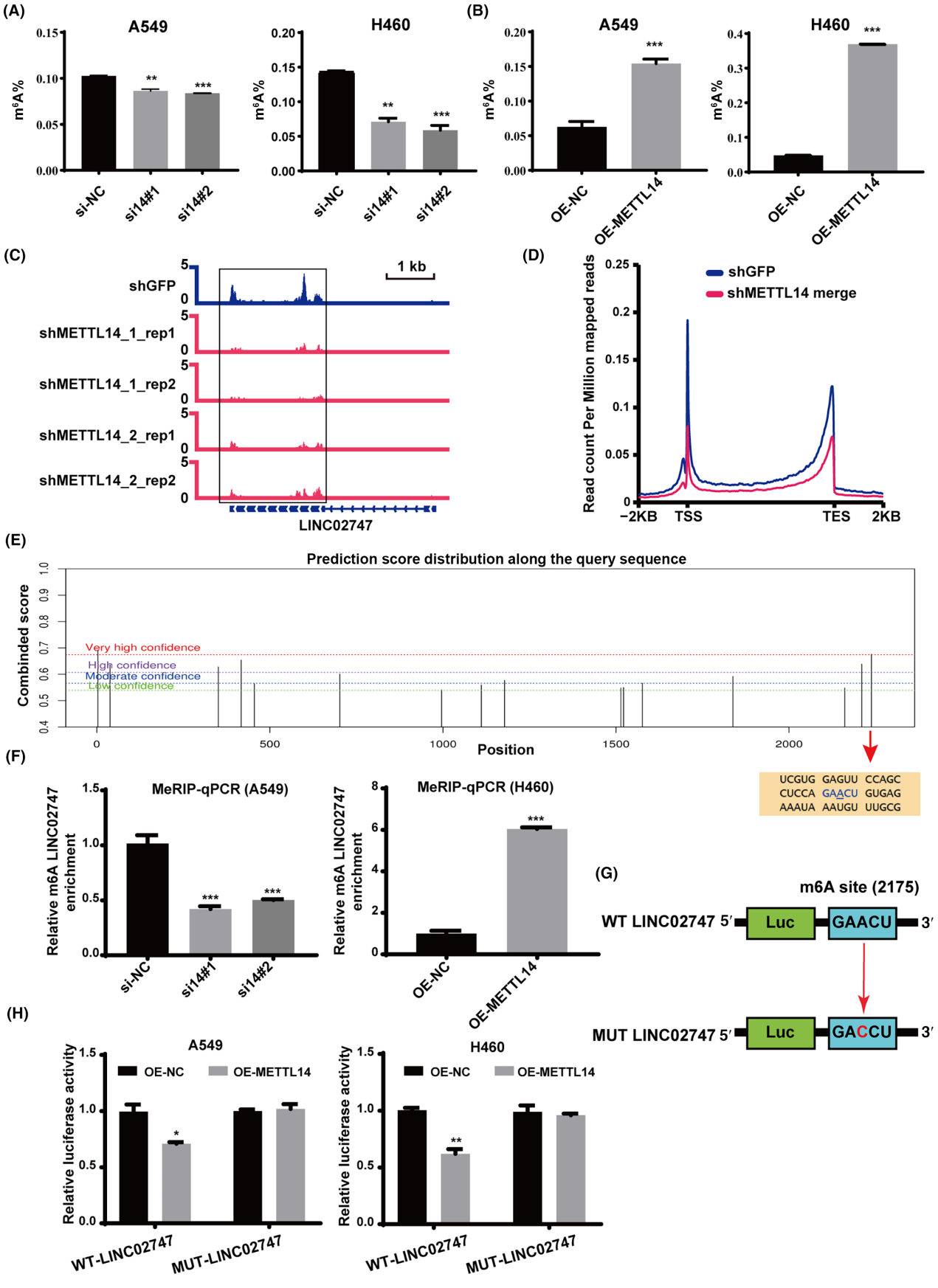
(A)
A549
H460
m6A%
si-NC
si14#1
si14#2
(B)
A549
H460
OE-NC
OE-METTL14
(C)
1 kb
shGFP
shMETTL14_1_rep1
shMETTL14_1_rep2
shMETTL14_2_rep1
shMETTL14_2_rep2
LINC02747
(D)
shGFP
shMETTL14 merge
Read count Per Million mapped reads
−2KB
TSS
TES
2KB
(E)
Prediction score distribution along the query sequence
Combined score
Very high confidence
High confidence
Moderate confidence
Low confidence
Position
UCGUG GAGUU CCAGC
CUCCA GAACU GUGAG
AAAUA AAUGU UUGCG
(F)
MeRIP-qPCR (A549)
MeRIP-qPCR (H460)
Relative m6A LINC02747 enrichment
(G)
m6A site (2175)
WT LINC02747 5′
Luc
GAACU
3′
MUT LINC02747 5′
GACCU
(H)
A549
H460
Relative luciferase activity
WT-LINC02747
MUT-LINC02747

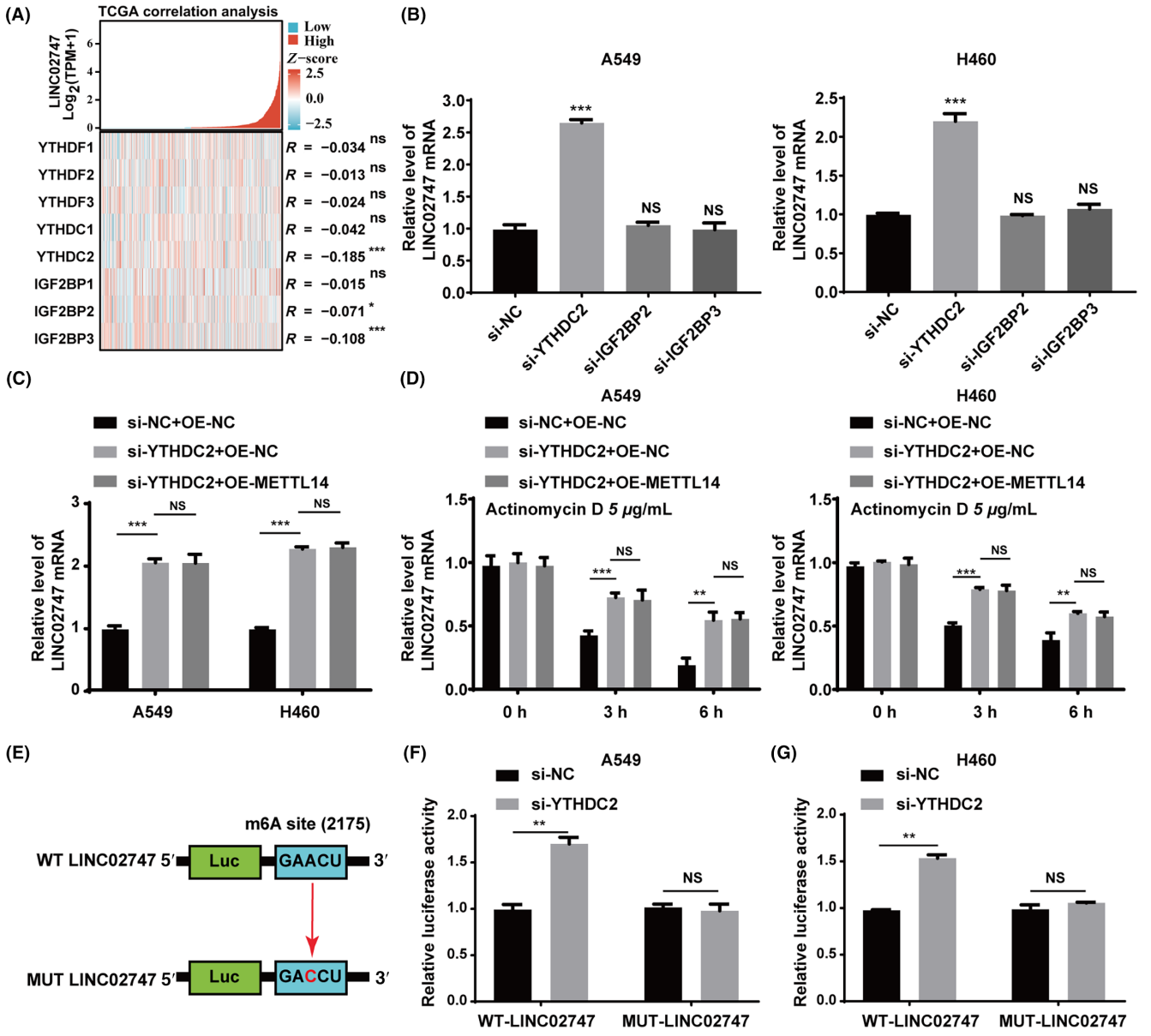

FIGURE 6 Overexpression of METTL14 accelerated the degradation of LINC02747 mRNA via a m^{6}A-YTHDC2-dependent pathway. (A) TCGA database to analyze the correlation between LINC02747 and reader proteins. (B) The mRNA levels of LINC02747 after knockdown of YTHDC2, IGF2BP2, and IGF2BP3 in NSCLC cells. (C) Regulation of LINC02747 mRNA expression by METTL14 and YTHDC2. (D) Degradation rate of LINC02747 in NSCLC cells after YTHDC2 interference and overexpression of METTL14. (E) The schematic shows the methylation site on LINC02747 and the site at which it was mutated. (F, G) Dual luciferase reporter assay of LINC02747 and YTHDC2 in NSCLC cells. Error bars = mean ± SD. $^{**}P < 0.01$, $^{***}P < 0.001$.

was conducted to confirm that LINC02747 was upregulated after YTHDC2 knockdown, whereas overexpression of METTL14 in the presence of YTHDC2 silencing resulted in unchanged LINC02747 expression (Figure 6C).

Subsequently, we investigated if YTHDC2 impacts the stability of LINC02747 through m^{6}A modification. Our study results indicated that under actinomycin D treatment, the knockdown of YTHDC2 leads to a slower degradation rate of LINC02747 in NSCLC cells. Moreover, on YTHDC2 silencing, overexpression of METTL14 did not alter the degradation rate of LINC02747 (Figure 6D). Additionally, we created a mutant version of LINC02747 with an altered m^{6}A binding site, preventing m^{6}A modification, for further analysis in luciferase reporter assays (Figure 6E). The results showed that si-YTHDC2 transfection significantly increased the luciferase activity in A549 and H460 cells with the wild-type LINC02747 sequence, but there was no noticeable change in luciferase activity in cells with the mutant LINC02747. These results imply that YTHDC2 is capable of interacting with the LINC02747 transcript, promoting its degradation by specifically targeting and binding to the m^{6}A sites within the transcript. Interestingly, the

analysis of the GEPIA database revealed that METTL14 was significantly positively correlated with YTHDC2 in NSCLC tissues (Figure S4E). Moreover, overexpression of METTL14 in NSCLC cell lines could increase YTHDC2 expression (Figure S4F). Overall, these results demonstrated that the m^{6}A "writer" METTL14-induced m^{6}A process inhibits LINC02747 expression through m^{6}A reader YTHDC2-dependent RNA degradation.

3.7 | KDM5B-mediated demethylation of H3K4me3 inhibited METTL14 transcription

To uncover the process underlying the downregulated expression of METTL14 in NSCLC, we analyzed H3K4me3 in ChIP sequencing (ChIP-seq) datasets and observed markedly lower accumulation of H3K4me3 at the METTL14 promoter region in NSCLC cells than in normal lung cells (Figure 7A). In addition, we found attenuated H3K4me3 modification signaling in the promoter region of the gene in NSCLC A549 and Calu-3 cells relative to that in the negative control cell line BEAS-2B (Figure 7B). Present research suggests that the majority of H3K4 trimethylation, encompassing the extensive H3K4me3 domain, is catalyzed by the KMT2F and KMT2G complexes,[14,15] whereas KDM5A-D catalyzes H3K4me3 demethylation and represses gene transcription by reducing H3K4 methylation.[16,17] Utilizing the GEPIA database, we examined KDM5A-D and KMT2F-G mRNA levels in TCGA-LUAD and TCGA-LUSC cohorts, discovering a significant upregulation of KDM5B mRNA in both LUAD and LUSC (Figure S5A). This increase in KDM5B mRNA was also observed in our NSCLC cohort, confirming the TCGA database findings (Figure S5B). To analyze the demethylation effect of KDM5B, we utilized the ChIPBase database to determine potential targets regulated by KDM5B. This led us to identify a possible KDM5B binding site located 89 bp downstream of METTL14 (Figure 7C). We then transfected specific siRNAs into A549 and H460 cells (Figures 7D and S5C) and observed that suppressing KDM5B resulted in a marked increase in both H3K4me3 protein expression and METTL14 RNA and protein levels (Figure 7E,F). Additionally, treatment with a KDM5B inhibitor (AS-8351) notably elevated METTL14 expression (Figure 7G,H). Furthermore, ChIP analysis further revealed that the METTL14 promoter had high levels of KDM5B binding and H3K4me3 signals, and inhibiting KDM5B led to an increased accumulation of H3K4me3 at this site (Figure 7I). The primer sequences of the METTL14 promoter region are shown in Table S4. More importantly, the results of the dual-luciferase reporter assay demonstrated that the luciferase activity of A549 and H460 cells transfected with wild-type METTL14 sequences was significantly increased after transfection with si-KDM5B, whereas there was no significant change in the luciferase activity of cells transfected with mutant METTL14 (Figure 7J,K). Our findings suggest that the reduction of histone H3K4me3 in the METTL14 promoter region due to KDM5B activity might be responsible for the decreased levels of METTL14.

3.8 | KDM5B upregulates the expression of LINC02747 by suppressing the expression of METTL14

Finally, we investigated the interactions among METTL14, KDM5B, and LINC02747 in NSCLC cells. Our qRT–PCR findings revealed that the overexpression of METTL14 led to a decrease in LINC02747 mRNA levels, while the upregulation of KDM5B enhanced the mRNA expression of LINC02747 (Figure 8A,B). Furthermore, Northern blot analysis revealed that elevated levels of KDM5B effectively counteracted the inhibitory impact of METTL14 on LINC02747 expression (Figure 8C). These findings suggest that KDM5B upregulates the expression of LINC02747 by inhibiting the transcriptional activity of METTL14 in NSCLC cells.

4 | DISCUSSION

NSCLC represents a prevalent subtype of lung cancer, characterized by a variety of pathological features. At present, NSCLC patients generally have a low overall survival rate, underscoring the necessity for deeper understanding of its underlying mechanisms and the discovery of potential biomarkers.[18–20] METTL14, a key element of the N^6-methyltransferase complex, has been implicated in diseases such as diabetic cardiomyopathy,[21] atherosclerosis,[22] and diabetic disease.[23] In this study, we noted a marked reduction in METTL14 levels in both NSCLC tissues and cell lines. Patients with low METTL14 expression levels had poor prognoses. Knockdown of METTL14 decreased m^{6}A abundance in NSCLC cells, while overexpression of METTL14 increased m^{6}A abundance. Furthermore, we discovered that downregulation of METTL14 expression contributed to the enhancement of the malignant phenotype in NSCLC cells. These findings align with

FIGURE 7 KDM5B-mediated demethylation of H3K4me3 inhibited METTL14 transcription. (A) Examination of H3K4me3 ChIP-seq data within the promoter region of METTL14 in NSCLC cells and lung epithelial cells. (B) H3K4me3 signaling analysis of gene promoter regions in NSCLC cells and lung epithelial cell. (C) Prediction of KDM5B and METTL14 binding sites using the ChIPBase database. (D) Detection of knockdown of KDM5B protein levels in NSCLC cells. (E) The mRNA expression level of METTL14 after KDM5B knockdown. (F) The protein levels of METTL14 and H3K4me3 after KDM5B knockdown. (G) The mRNA levels of METTL14 after treatment with the KDM5B inhibitor AS-8351 (5 μM). (H) METTL14 and H3K4me3 protein levels after treatment with AS-8351 at a concentration of 5 μM. (I) ChIP assays measured the binding of KDM5B and the enrichment of H3K4me3 at the METTL14 promoter in NSCLC cells treated with either AS-8351 or DMSO. (J) Sketch of METTL14 promoter region dual luciferase reporter vector construction. (K) Dual luciferase reporter assay for KDM5B targeting METTL14. Error bars = mean ± SD. $^{**}P < 0.01$, $^{***}P < 0.001$.

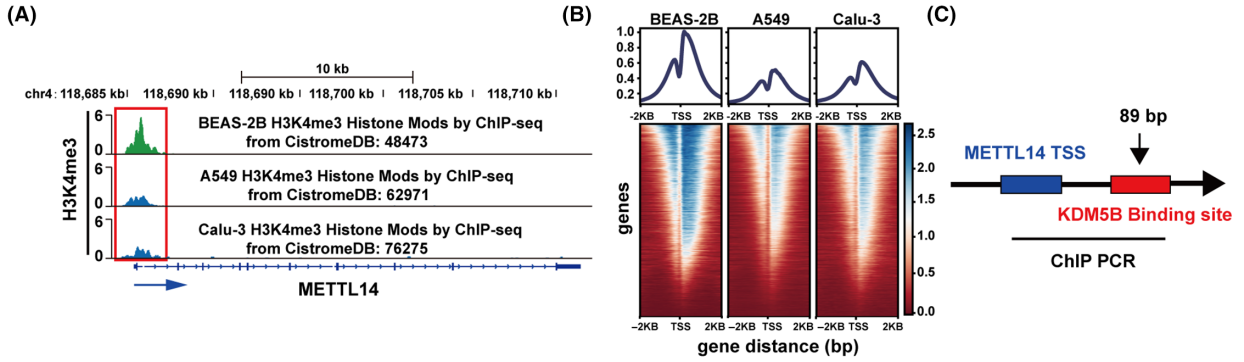
(A)
10 kb
chr4: 118,685 kb 118,690 kb 118,690 kb 118,700 kb 118,705 kb 118,710 kb
H3K4me3
BEAS-2B H3K4me3 Histone Mods by ChIP-seq from CistromeDB: 48473
A549 H3K4me3 Histone Mods by ChIP-seq from CistromeDB: 62971
Calu-3 H3K4me3 Histone Mods by ChIP-seq from CistromeDB: 76275
METTL14
(B)
BEAS-2B
A549
Calu-3
genes
gene distance (bp)
(C)
89 bp
METTL14 TSS
KDM5B Binding site
ChIP PCR

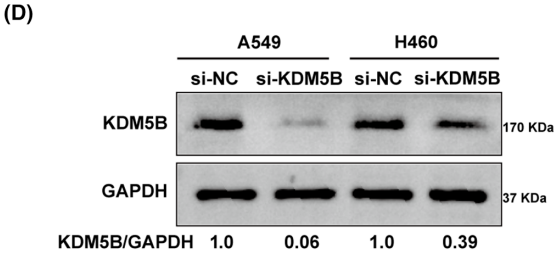
(D)
A549
H460
si-NC si-KDM5B si-NC si-KDM5B
KDM5B
GAPDH
170 KDa
37 KDa
KDM5B/GAPDH 1.0 0.06 1.0 0.39

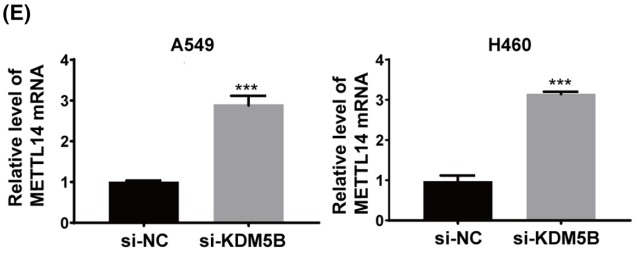
(E)
A549
H460
Relative level of METTL14 mRNA
si-NC si-KDM5B

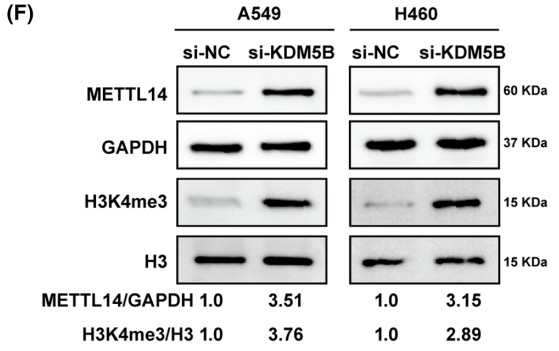
(F)
A549
H460
si-NC si-KDM5B si-NC si-KDM5B
METTL14
GAPDH
H3K4me3
H3
60 KDa
37 KDa
15 KDa
15 KDa
METTL14/GAPDH 1.0 3.51 1.0 3.15
H3K4me3/H3 1.0 3.76 1.0 2.89

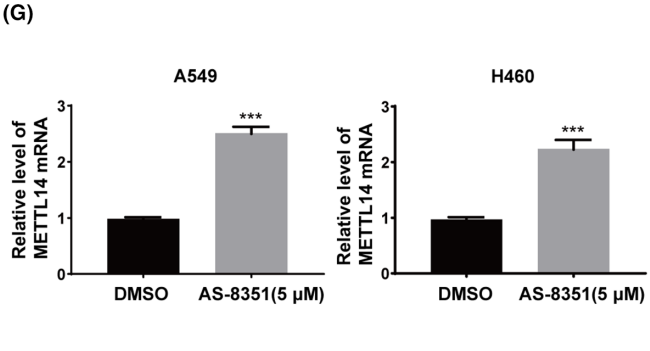
(G)
A549
H460
Relative level of METTL14 mRNA
DMSO AS-8351(5 μM)

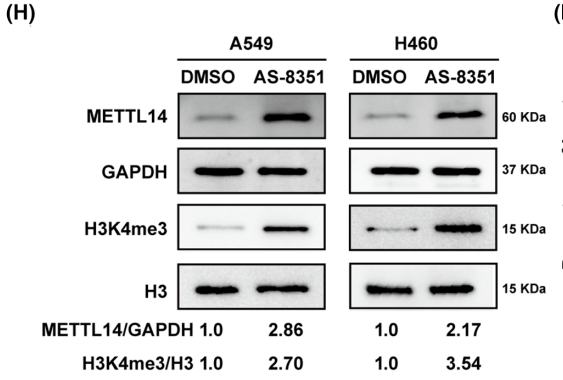
(H)
A549
H460
DMSO AS-8351 DMSO AS-8351
METTL14
GAPDH
H3K4me3
H3
60 KDa
37 KDa
15 KDa
15 KDa
METTL14/GAPDH 1.0 2.86 1.0 2.17
H3K4me3/H3 1.0 2.70 1.0 3.54

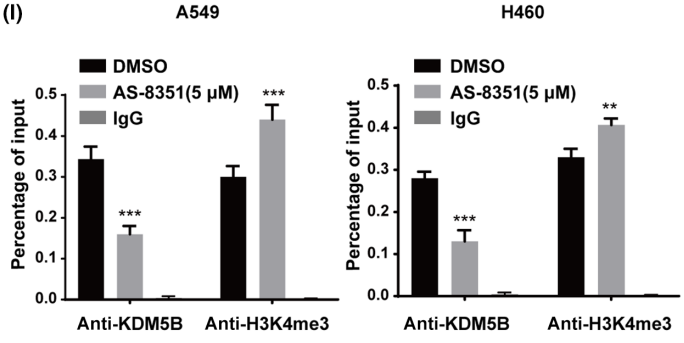
(I)
A549
H460
DMSO
AS-8351(5 μM)
IgG
Percentage of input
Anti-KDM5B Anti-H3K4me3

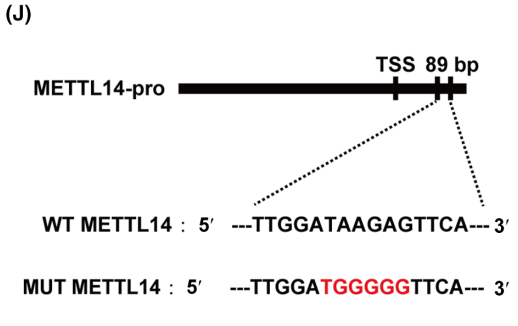
(J)
METTL14-pro
TSS 89 bp
WT METTL14 : 5′ ---TTGGATAAGAGTTCA--- 3′
MUT METTL14 : 5′ ---TTGGATGGGGGTTCA--- 3′

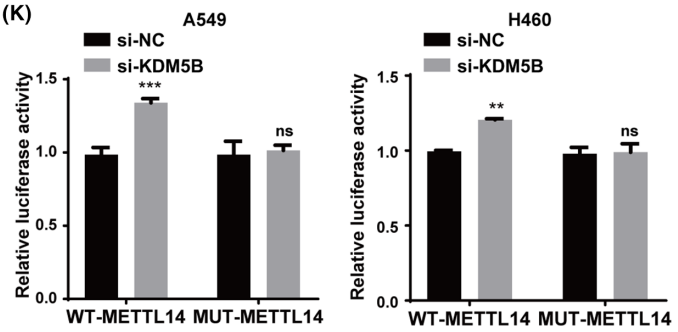
(K)
A549
H460
si-NC
si-KDM5B
Relative luciferase activity
ns
WT-METTL14 MUT-METTL14

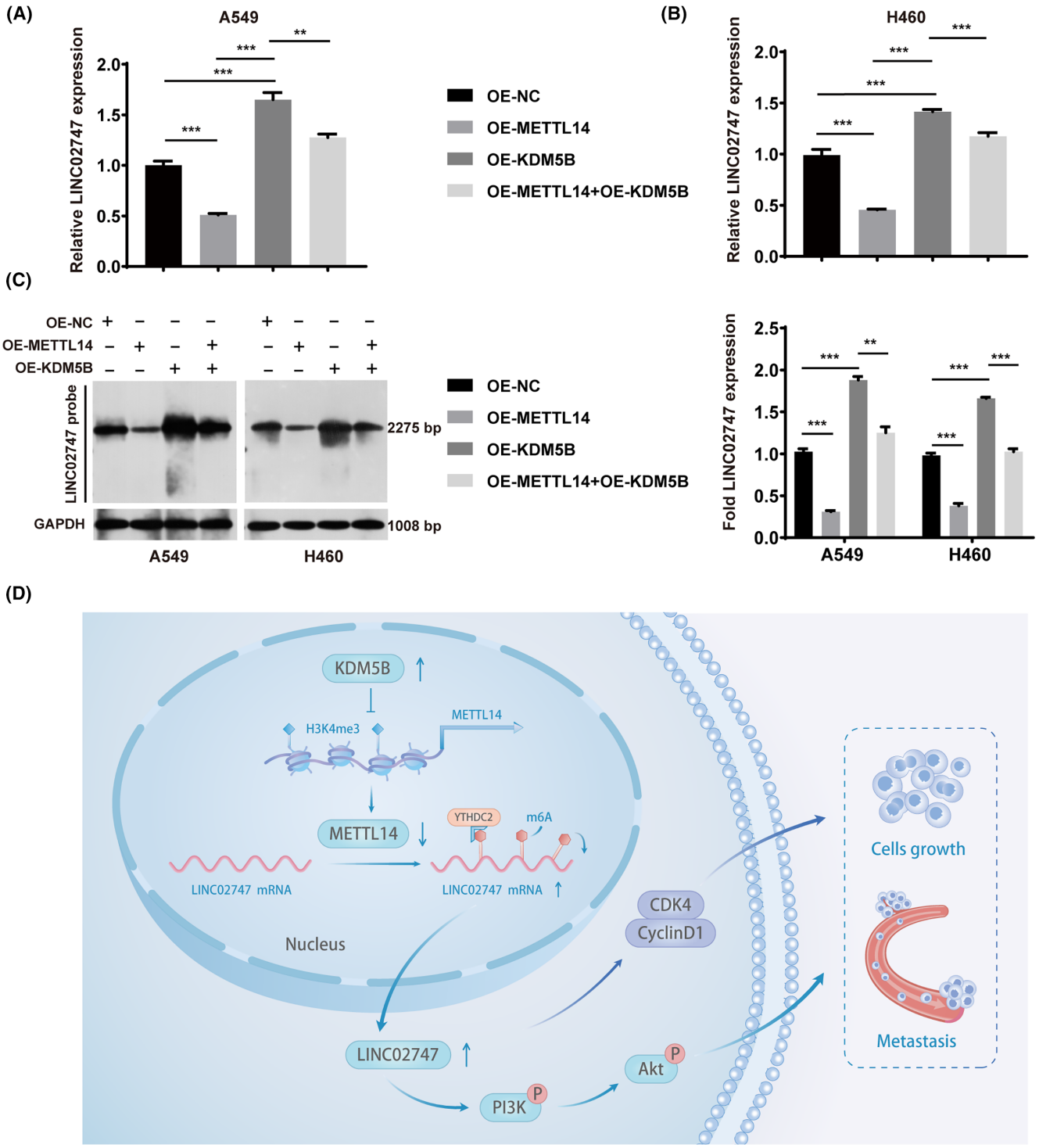

FIGURE 8 KDM5B upregulates the expression of LINC02747 by suppressing the expression of METTL14. (A, B) Expression of LINC02747 was analyzed after overexpression of both METTL14 and KDM5B. (C) Northern blot was used to analyze the regulation of LINC02747 expression by KDM5B through METTL14. (D) Graphic abstract of METTL14 regulating the malignant phenotype of NSCLC. Error bars = mean ± SD. $^{**}P < 0.01$, $^{***}P < 0.001$.

previous studies reporting low METTL14 expression in lung cancer tissues and cells.[24,25] However, there are also reports of increased expression of METTL14 in NSCLC cells.[26,27] This discrepancy may be attributed to several factors. First, differences in experimental design could lead to inconsistent results. For instance, variations in cell lines, animal models, or experimental conditions utilized by different laboratories may yield diverse outcomes. Secondly, the source and quantity of samples may influence the results. Additionally, differences in technical platforms, such as the choice of gene expression analysis methods and data processing and analysis approaches, may

contribute to observed expression pattern discrepancies. Moreover, tumor heterogeneity and complexity could be among the reasons for the differences in results. Distinct tumor subtypes or pathological features might lead to varying expression patterns. Furthermore, the complexity of cell interactions and signaling pathways in the tumor microenvironment could influence the expression and function of METTL14.

Recently, the role of the m^{6}A RNA modification, a key facet of posttranscriptional regulation, in regulating the expression of lung cancer genes has attracted increased amounts of attention.[28,29] we confirmed that METTL14 negatively regulates LINC02747, which is subject to m^{6}A methylations facilitated by METTL14. Additionally, we observed that silencing METTL14 promoted the malignant phenotype of NSCLC cells by upregulating CDK4/cyclin D1 complex expression and activating the PI3K/Akt signaling pathway, whereas knockdown of LINC02747 attenuated this effect. Previous studies have indicated that LINC02747 enhances the malignancy of clear cell renal cell carcinoma.[12] In our study, we observed a notable increase in LINC02747 expression in both NSCLC tissues and cells. Silencing LINC02747 reduces NSCLC cell proliferation and migration by inhibiting the PI3K/Akt pathway. The m^{6}A reader is the ultimate determinant of the post-transcriptional effects of m^{6}A modification on RNA. YTHDC2, considered the final member of the YTH protein family, functions as a reader to suppress hepatic steatosis[30] and lung adenocarcinoma.[31] Mechanistically, YTHDC2 binds to m^{6}A-modified mRNA, subsequently reducing its mRNA stability.[32] Our results showed that knockdown of YTHDC2 resulted in upregulation of LINC02747 in NSCLC cells, whereas METTL14 did not result in decreased LINC02747 expression in the presence of YTHDC2 knockdown. The results confirmed that the m^{6}A reader was the protein that ultimately determined the post-transcriptional effect of m^{6}A modification on RNA. Additionally, we found that YTHDC2 binds directly to the A site on the LINC02747 GAACU motif. Taken together, these findings suggest that downregulation of METTL14 expression upregulates the expression of LINC02747-mediated CDK4/CyclinD1 complex and activates the PI3K/Akt signaling pathway, leading to the promotion of a malignant phenotype in NSCLC cells. Moreover, our findings revealed that downregulated METTL14 expression in NSCLC cells led to a decrease in m^{6}A modification. This reduction hindered the ability of YTHDC2 to recognize and bind to LINC02747, consequently enhancing the stability of LINC02747 mRNA and increasing its expression levels.

Epigenetic mechanisms can modulate gene expression in the context of cancer development, exerting regulatory control at multiple cellular junctures, including the transcriptional and post-transcriptional stages.[33,34] Notably, the state of histone modification may influence the addition or removal of m^{6}A marks. For instance, in mouse embryonic stem cells, m^{6}A modifications tend to be concentrated near peaks of H3K36me3 and show a global decrease when H3K36me3 levels in the cells are diminished.[35] In cholangiocarcinoma cells, the histone acetyltransferase p300 regulates METTL16 gene expression via H3K27ac.[36] KDM5B, a highly conserved member of the H3K4 demethylase family, is frequently overexpressed in malignant tumors.[37,38] Since KDM5 enzymes, including KDM5B, play a role in erasing the epigenetic signature of H3K4me3, their dysregulation in cancer cells could contribute to epigenetic flexibility and disturb the intrachromosomal equilibrium. This disruption can potentially facilitate the development of tumors.[39] We analyzed publicly available ChIP-seq data and found that H3K4me3 enrichment of the METTL14 promoter was significantly reduced in NSCLC cell lines compared to normal lung epithelial cells. Interestingly, inhibition of KDM5B expression resulted in elevated levels of H3K4me3 and METTL14 expression. In addition, ChIP–qPCR results showed that inhibition of KDM5B increased H3K4me3 enrichment in the METTL14 promoter region in NSCLC cells. These findings demonstrate that demethylation of H3K4me3 in the promoter region of METTL14 by KDM5B represses its transcription, leading to its downregulated expression in NSCLC. In addition, upregulation of KDM5B reversed the inhibitory effect of METTL14 on LINC02747 expression in NSCLC cells.

Taken together, our study highlights the critical importance of m^{6}A modification mediated by METTL14 in the progression of human NSCLC. We confirmed that METTL14 epigenetically suppressed LINC02747 expression through an m^{6}A-YTHDC2-dependent mechanism. Subsequent investigations demonstrated that the KDM5B can hinder METTL14 transcription through histone modification and upregulate LINC02747 expression (Figure 8D). Additionally, METTL14 acted as a prognostic marker for the prognosis of NSCLC patients. These results might provide clues for future clinical therapeutic strategies for NSCLC, and more studies are urgently needed to reveal the complete m^{6}A regulatory network.

AUTHOR CONTRIBUTIONS

Jiemin Wang: Data curation; investigation; methodology; writing – original draft; writing – review and editing. **Shu Wang:** Data curation; software; validation; writing – original draft; writing – review and editing. **Haopeng Yang:** Data curation; investigation; methodology. **Ruixuan Wang:** Data curation; formal analysis; software. **Kesong Shi:** Data curation; investigation. **Yueshi Liu:** Data curation; validation. **Le Dou:** Investigation. **Haiquan Yu:** Funding acquisition; project administration; resources.

ACKNOWLEDGMENTS

We thank all members of our laboratory for their assistance and the biotrainee platform for sharing knowledge about bioinformatics.

FUNDING INFORMATION

We would like to acknowledge the funding from the Science and Technology Program of the Joint Fund of Scientific Research for the Public Hospitals of Inner Mongolia Academy of Medical Sciences (2023GLLH0037), and the Key Technology Research Plan Project of Inner Mongolia Autonomous Region (2021GG0153) to H.Y.

CONFLICT OF INTEREST STATEMENT

The authors declare no conflict of interest.

ETHICS STATEMENTS

Approval of the research protocol by an Institutional Review Board: The study of human sample was approved by the Ethics Committee of Shanghai Outdo Biotech Company, Shanghai, China.

Informed Consent: Informed consent was obtained from all patients in accordance with a protocol approved by the ethics review board of Shanghai Outdo Biotech (approval no.: YB M-05-02). Written informed consent was obtained from each subject.

Registry and the Registration No. of the study/trial: N/A.

Animal Studies: Experimental protocols were approved by the Institutional Animal Care and Use Committee of Inner Mongolia University (IMU-mouse-2021-046). All animals were managed and treated according to the guidelines of Inner Mongolia University.

ORCID

Haiquan Yu https://orcid.org/0000-0002-2580-0878

REFERENCES

1. Relli V, Trerotola M, Guerra E, Alberti S. Abandoning the notion of non-small cell lung cancer. *Trends Mol Med*. 2019;25(7):585-594. doi:10.1016/j.molmed.2019.04.012
2. Yang Q, Wang M, Xu J, et al. LINC02159 promotes non-small cell lung cancer progression via ALYREF/YAP1 signaling. *Mol Cancer*. 2023;22(1):122. doi:10.1186/s12943-023-01814-x
3. Shi K, Sa R, Dou L, et al. METTL3 exerts synergistic effects on m^{6}A methylation and histone modification to regulate the function of VGF in lung adenocarcinoma. *Clin Epigenetics*. 2023;15(1):153. doi:10.1186/s13148-023-01568-9
4. Bove G, Amin S, Babaei M, et al. Interplay between m^{6}A epitranscriptome and epigenome in cancer: current knowledge and therapeutic perspectives. *Int J Cancer*. 2023;153(3):464-475. doi:10.1002/ijc.34378
5. Wang X, Lu Z, Gomez A, et al. N^6-methyladenosine-dependent regulation of messenger RNA stability. *Nature*. 2014;505(7481):117-120. doi:10.1038/nature12730
6. Huang H, Weng H, Chen J. m^{6}A modification in coding and non-coding RNAs: roles and therapeutic implications in cancer. *Cancer Cell*. 2020;37(3):270-288. doi:10.1016/j.ccell.2020.02.004
7. Schwartz S, Mumbach MR, Jovanovic M, et al. Perturbation of m^{6}A writers reveals two distinct classes of mRNA methylation at internal and 5′ sites. *Cell Rep*. 2014;8(1):284-296. doi:10.1016/j.celrep.2014.05.048
8. Wang T, Kong S, Tao M, Ju S. The potential role of RNA N^6-methyladenosine in cancer progression. *Mol Cancer*. 2020;19(1):88. doi:10.1186/s12943-020-01204-7
9. Ma JZ, Yang F, Zhou CC, et al. METTL14 suppresses the metastatic potential of hepatocellular carcinoma by modulating N^6-methyladenosine-dependent primary microRNA processing. *Hepatology*. 2017;65(2):529-543. doi:10.1002/hep.28885
10. Sherr CJ, Beach D, Shapiro GI. Targeting CDK4 and CDK6: from discovery to therapy. *Cancer Discov*. 2016;6(4):353-367. doi:10.1158/2159-8290.Cd-15-0894
11. Tchakarska G, Sola B. The double dealing of cyclin D1. *Cell Cycle*. 2020;19(2):163-178. doi:10.1080/15384101.2019.1706903
12. Ju X, Sun Y, Zhang F, Wei X, Wang Z, He X. Long non-coding RNA LINC02747 promotes the proliferation of clear cell renal cell carcinoma by inhibiting miR-608 and activating TFE3. *Front Oncol*. 2020;10:573789. doi:10.3389/fonc.2020.573789
13. Allis CD, Jenuwein T. The molecular hallmarks of epigenetic control. *Nat Rev Genet*. 2016;17(8):487-500. doi:10.1038/nrg.2016.59
14. Yang W, Ernst P. SET/MLL family proteins in hematopoiesis and leukemia. *Int J Hematol*. 2017;105(1):7-16. doi:10.1007/s12185-016-2118-8
15. Lee JH, Tate CM, You JS, Skalnik DG. Identification and characterization of the human Set1B histone H3-Lys4 methyltransferase complex. *J Biol Chem*. 2007;282(18):13419-13428. doi:10.1074/jbc.M609809200
16. Davie JR, Xu W, Delcuve GP. Histone H3K4 trimethylation: dynamic interplay with pre-mRNA splicing. *Biochem Cell Biol*. 2016;94(1):1-11. doi:10.1139/bcb-2015-0065
17. Guo X, Zhang Q. The emerging role of histone demethylases in renal cell carcinoma. *J Kidney Cancer VHL*. 2017;4(2):1-5. doi:10.15586/jkcvhl.2017.56
18. Chen Z, Fillmore CM, Hammerman PS, Kim CF, Wong KK. Non-small-cell lung cancers: a heterogeneous set of diseases. *Nat Rev Cancer*. 2014;14(8):535-546. doi:10.1038/nrc3775
19. Wang Y, Wang Y, Gu J, Su T, Gu X, Feng Y. The role of RNA m^{6}A methylation in lipid metabolism. *Front Endocrinol*. 2022;13:866116. doi:10.3389/fendo.2022.866116
20. Dai D, Wang H, Zhu L, Jin H, Wang X. N^6-methyladenosine links RNA metabolism to cancer progression. *Cell Death Dis*. 2018;9(2):124. doi:10.1038/s41419-017-0129-x
21. Meng L, Lin H, Huang X, Weng J, Peng F, Wu S. METTL14 suppresses pyroptosis and diabetic cardiomyopathy by downregulating TINCR lncRNA. *Cell Death Dis*. 2022;13(1):38. doi:10.1038/s41419-021-04484-z
22. Zheng Y, Li Y, Ran X, et al. Mettl14 mediates the inflammatory response of macrophages in atherosclerosis through the NF-κB/IL-6 signaling pathway. *Cell Mol Life Sci*. 2022;79(6):311. doi:10.1007/s00018-022-04331-0
23. Xu Z, Jia K, Wang H, et al. METTL14-regulated PI3K/Akt signaling pathway via PTEN affects HDAC5-mediated epithelial-mesenchymal transition of renal tubular cells in diabetic kidney disease. *Cell Death Dis*. 2021;12(1):32. doi:10.1038/s41419-020-03312-0
24. Li F, Zhao J, Wang L, Chi Y, Huang X, Liu W. METTL14-mediated miR-30c-1-3p maturation represses the progression of lung cancer via regulation of MARCKSL1 expression. *Mol Biotechnol*. 2022;64(2):199-212. doi:10.1007/s12033-021-00406-8
25. Mao J, Qiu H, Guo L. LncRNA HCG11 mediated by METTL14 inhibits the growth of lung adenocarcinoma via IGF2BP2/LATS1. *Biochem Biophys Res Commun*. 2021;580:74-80. doi:10.1016/j.bbrc.2021.09.083
26. Ji X, Wan X, Sun H, et al. METTL14 enhances the m^{6}A modification level of lncRNA MSTRG.292666.16 to promote the progression of non-small cell lung cancer. *Cancer Cell Int*. 2024;24(1):61. doi:10.1186/s12935-024-03250-3
27. Zhou Q, Lai X, Gao Y, Chen Q, Xu Y, Liu Y. METTL14 regulates PLAGL2/β-catenin signaling Axis to promote the development of nonsmall cell lung cancer. *J Oncol*. 2023;2023:4738586. doi:10.1155/2023/4738586
28. Chen M, Zhang Q, Zheng S, et al. Cancer-associated fibroblasts promote migration and invasion of non-small cell lung cancer cells via METTL3-mediated RAC3 m^{6}A modification. *Int J Biol Sci*. 2023;19(5):1616-1632. doi:10.7150/ijbs.79467
29. Jin D, Guo J, Wu Y, et al. m^{6}A demethylase ALKBH5 inhibits tumor growth and metastasis by reducing YTHDFs-mediated YAP expression and inhibiting miR-107/LATS2-mediated YAP activity in NSCLC. *Mol Cancer*. 2020;19(1):40. doi:10.1186/s12943-020-01161-1
30. Zhou B, Liu C, Xu L, et al. N^6-Methyladenosine reader protein YT521-B homology domain-containing 2 suppresses liver steatosis by regulation of mRNA stability of lipogenic genes. *Hepatology*. 2021;73(1):91-103. doi:10.1002/hep.31220
31. Ma L, Chen T, Zhang X, et al. The m^{6}A reader YTHDC2 inhibits lung adenocarcinoma tumorigenesis by suppressing SLC7A11-dependent antioxidant function. *Redox Biol*. 2021;38:101801. doi:10.1016/j.redox.2020.101801

32. Jiang X, Liu B, Nie Z, et al. The role of m^6A modification in the biological functions and diseases. *Signal Transduct Target Ther*. 2021;6(1):74. doi:10.1038/s41392-020-00450-x
33. Zhu J, Fu H, Wu Y, Zheng X. Function of lncRNAs and approaches to lncRNA-protein interactions. *Sci China Life Sci*. 2013;56(10):876-885. doi:10.1007/s11427-013-4553-6
34. Alqinyah M, Hooks SB. Regulating the regulators: epigenetic, transcriptional, and post-translational regulation of RGS proteins. *Cell Signal*. 2018;42:77-87. doi:10.1016/j.cellsig.2017.10.007
35. Huang H, Weng H, Zhou K, et al. Histone H3 trimethylation at lysine 36 guides m^6A RNA modification co-transcriptionally. *Nature*. 2019;567(7748):414-419. doi:10.1038/s41586-019-1016-7
36. Liu N, Zhang J, Chen W, Ma W, Wu T. The RNA methyltransferase METTL16 enhances cholangiocarcinoma growth through PRDM15-mediated FGFR4 expression. *J Exp Clin Cancer Res*. 2023;42(1):263. doi:10.1186/s13046-023-02844-5
37. Xhabija B, Kidder BL. KDM5B is a master regulator of the H3K4-methylome in stem cells, development and cancer. *Semin Cancer Biol*. 2019;57:79-85. doi:10.1016/j.semcancer.2018.11.001
38. He R, Xhabija B, Gopi LK, et al. H3K4 demethylase KDM5B regulates cancer cell identity and epigenetic plasticity. *Oncogene*. 2022;41(21):2958-2972. doi:10.1038/s41388-022-02311-z
39. Plch J, Hrabeta J, Eckschlager T. KDM5 demethylases and their role in cancer cell chemoresistance. *Int J Cancer*. 2019;144(2):221-231. doi:10.1002/ijc.31881

SUPPORTING INFORMATION

Additional supporting information can be found online in the Supporting Information section at the end of this article.

How to cite this article: Wang J, Wang S, Yang H, et al. Methyltransferase like-14 suppresses growth and metastasis of non-small-cell lung cancer by decreasing LINC02747. *Cancer Sci*. 2024;115:2931-2946. doi:10.1111/cas.16254